

工學碩士 學位論文

초소형 CMOS 대역통과필터 특성에 관한  
연구

An Extremely Miniaturized Two-stage Bandpass  
Filter

指導教授 姜仁鎬



2010年 6月

韓國海洋大學校 大學院

電波工學科

李尚明

# **An Extremely Miniaturized Two-stage**

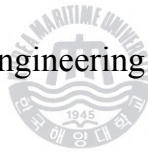
## **Bandpass Filter**

By Shang-Ming Li

Here is approved that this is the thesis submitted in partial  
satisfaction of the requirements for degree of

MASTER

in Radio Sciences and Engineering in the Graduate School of



Korea Maritime University

Approved by: Prof. Ki-Man Kim

Prof. Young Yun

Prof. In-Ho Kang

Committee in Charge

# Contents

<b>Contents</b> .....	<b>i</b>
<b>Nomenclature</b> .....	<b>ii</b>
<b>List of Figures</b> .....	<b>iii</b>
<b>Abstract</b> .....	<b>v</b>
<b>CHAPTER 1 Introduction</b> .....	<b>1</b>
1.1 An introduction to the filters at present .....	1
1.2 Organization of the thesis.....	4
<b>CHAPTER 2 The Bandpass Filter Design Theory</b> .....	<b>6</b>
2.1 Size reduction method .....	6
2.2 The two-stage filter .....	11
2.3 The inter-stage signal line enhancement method .....	13
<b>CHAPTER 3 The Simulation , fabrication and results analysis..</b>	<b>14</b>
3.1 The inter-stage signal line improvement .....	14
3.2 Simulation and fabrication.....	17
3.3 The quality factor effect on the resonance frequency shift.....	25
<b>CHAPTER 4 Conclusion</b> .....	<b>32</b>
<b>References</b> .....	<b>34</b>
<b>Acknowledgement</b> .....	<b>37</b>

## Nomenclature

$f$ :	Frequency
$Q$ :	Quality factor
$Z_0$ :	Characteristic impedance
$Z_{0e}$ :	Even-mode characteristic impedance
$Z_{0o}$ :	Odd-mode characteristic impedance
$\omega$ :	Angular frequency
$\theta$ :	Electrical length
$C$ :	Capacitance
$L$ :	Inductance
$R$ :	Resistance
$S_{11}$ :	Return loss
$S_{21}$ :	Insertion loss



## List of Figures

- Fig.2.1 Quarter-wave transmission line (a) and the shortened transmission line with lump capacitors(b)
- Fig. 2.2 Diagonally shorted coupled lines (a) and the equivalent circuit of the coupled lines (b)
- Fig. 2.3 A shortened transmission line with artificial resonance circuits
- Fig.2.4 The equivalent circuit substituted by the coupled lines' equivalent
- Fig. 2.5 The final equivalent circuit of the miniaturized quarter-wave transmission line
- Fig. 2.6 The two-stage bandpass filter
- Fig. 3.1 An extremely miniaturized two-stage bandpass filter
- Fig. 3.2 The series resistance is substituted by the shunt conductance.
- Fig. 3.3The inter-stage signal line of the 2-stage bandpass filter (a) without ground plane (b) with ground plane.
- Fig. 3.4 Structure of the two-stage bandpass filters (a) the original filter without ground plane (b) the improved with ground plane.
- Fig. 3.5 Photograph of the fabricated six-layer bandpass filters with 6 layers (a) the original filter without ground plane (b) the improved with ground plane
- Fig. 3.6 Electric field distributions for original connection part (a) and improved connection part(b) .
- Fig. 3.7Vector electric field distributions for original connection part (a) and improved connection part (b)
- Fig. 3.8 The simulated results of the circuits with (a) 1 layer and (b) 6 layers.
- Fig. 3.9 The measured results of the circuits with 6 layers.
- Fig. 3.10 The Equivalent circuit of the resonator

Fig. 3.11 The logarithm of  $\frac{\Delta w}{w_0}$  versus the  $Q_L$  factor

Fig. 3.12 The simulated and the measured results of the improved circuit with one-layer coupled lines (a) and six-layer coupled lines (b)



# Abstract

Bandpass filters are key components in RF/microwave communication systems. As the system goes smaller and lighter, size reduction becomes more and more important. In addition, impedance matching and high performance is also crucial to a communication system. Thus, a two-stage bandpass filter with both small size and automatically matching is more desirable.

In this thesis, a novel miniaturized CMOS bandpass filter will be introduced. It is based on the structure of diagonally short-ended coupled line with loaded capacitors for size reduction and using multilayer conductors for high quality factor. In this structure, the ground plane is encapsulated around the filter, which enables it avoid the coupling to other basic components in the transceiver system. In addition, as another major advantage, it was proven to have an impedance matching automatically. The greater difference between the simulation and measurement in CMOS fabrication is also analysed and it will be proven to be caused by transmission losses and quality factors in the lossy distributed inductor of shunt resonator.

Design equations and method will be fully explained in this thesis. A lot of simulated results and measured results are also presented. The method of enhancing the performance of the bandpass filters and automatically impedance matching will be described. Four kinds of circuits which based on the MagnaChip 0.18 $\mu\text{m}$  process are fabricated.

Many simulated and measured data are collected and provided here to show the advantages of the proposed bandpass filter.





## **CHAPTER 1 Introduction**

Bandpass filters are important components in wireless communication systems, used for filtering the signals that are not wanted and providing transmission at the desired frequency. Due to their widely application in the wireless communication systems, the filters with small size, low cost and high performance are seriously attractive. The fact that communication systems go smaller and lighter is another motivation of the filter design. If the bandpass filter can be integrated with active components by inserting all external filter components into the transceiver chip, the cost of the system will be greatly reduced.

In this thesis a two-stage bandpass filter based on the structure which using short-ended coupled line with lumped capacitors is introduced. The compacted size and the surrounding ground structure enable it can be inserted into the transceiver systems. In addition, the high quality factor (Q) and the automatically impedance matching are other advantages. The filter can be fabricated using the standard CMOS process.

### **1.1 An introduction to the filters at present**

To meet the demand of some certain applications, the size reduction of filter is of primary importance. Smaller filters are desirable, even

though reducing the size of a filter generally leads to reducing performance. Many efforts have been done on reducing the size of the conventional filters. So far, numerous new filter configurations become possible. For instance, the miniature dual-mode resonator filters [1]-[3] can reduce the filter by half. Slow-wave resonator filter [4], [5] is another effective approach in reducing the size of the bandpass filter by making use of the slow-wave effect in periodic structures. Combine filters using low temperature co-fired ceramic (LTCC) or ceramic materials with the multi-layer technology can be an effective size reduction method [6], [7]. But conventionally the electrical length has been recommended by 45 degree. There are many other size reduction methods such as the hairpin resonator filters [8] and the step impedance filters (SIR) [9]-[11]. All these methods mentioned above can achieve relatively compact bandpass filter size. But still take up a large circuit space. It is inconvenient for the system integration.

Recently, CMOS bandpass filters for a single RF transceiver chip have been driven by reducing the cost and decreasing the RF system design time. A CMOS-based integrated filter using lumped inductors was fabricated [12]. However, the filter design is not convenient and has limitations since the lumped inductor has a complex equivalent circuit and low self-resonance frequency. Active bandpass filter can be an effective approach on size reduction. Great efforts have been done in the area of on-chip active bandpass filter. However, their uptake for commercial RF front end designs is limited owing to the poor performances resulting from the low quality factor of monolithic spiral inductors. These inductors suffer inherently from a variety of energy dissipation mechanisms. The

Ohmic loss is unavoidable as the primary inductor current flows through the thin metals of the spiral. Displacement current losses within the dielectric between the inductor and the underlying semiconductor substrate, and eddy current losses within the silicon (Si) substrate [13], [14]. Many approaches have been proposed to solve or alleviate these lossy inductor issues. Such as use patterned ground shields with polysilicon [15] and multi-metal spiral inductors [16], [17]. However, the realization of high quality factors ( $>10$ ) still remains a challenge using the standard CMOS process. A series of active filters could be used to compensate for the inductor losses, but this approach suffers with other problems such as limited dynamic range, narrow bandwidth, high intermodulation distortion, high noise figure and poor in-band flatness. It has been reported that the system performance using the silicon-on-insulator (SOI) process (where inductors with quality factors  $Q > 20$  are attainable) was comparable to that of a conventional low noise amplifier with an off-chip bandpass filter [18]. However, it is not usual for a single chip transceiver to include an integrated bandpass filter. In spite of its small silicon area and good insertion loss of the active filters, the active circuit has a drawback inherent that it has nonlinear and poor noise characteristics and consumes the DC power. Until recently, there have been limited publications regarding low GHz band, CMOS passive filters.

On the other side, these filters published by CMOS technology have suffered from inherent losses with silicon substrate. Especially, these losses with spiral inductors are inclined to cause the center frequency to shift to the lower frequency. For the frequency tuning in the active BPFs, the master-slave (M/S) tuning[19], self-tuning, such as the correlated tuning loop[20] or orthogonal reference tuning technology [21] was

implemented. A ground plane on metal in BPF with the standard multilayer metal CMOS technology was employed to address these frequency shifting, thereby, minimizing the electrical field leakage into the silicon substrate[22]. The greater difference between the simulation and measurement in CMOS fabrication was not analyzed until now.

In this thesis, a novel bandpass filter was designed using the diagonally short-ended coupled line with loaded lumped capacitor for size reduction. The structure is simple and it is convenient to integrate with active components. In order to have an excellent impedance matching, two-stage structure is used. An extra ground plane is inserted into below the signal line between two filters in the multilayers to enhance the performance of the filter. The simulation result confirmed that the filter with ground plane below the inter-stage line has a better performance than the one without ground plane. The center frequency shifts will be theoretically proven to be caused by transmission losses and quality factors in the lossy distributed inductor of the shunt resonator. These approaches will be verified by the measurements of BPFs with two kinds of quality factors.

## **1.2 Organization of the thesis**

The contents of the thesis are as follows:

Chapter 1 depicts the background and purpose of this work and give a briefly introduces to the outline of the thesis.

Chapter 2 introduces the design theory of the bandpass filters.

Chapter 3 the simulation and the measurement results are plotted, including simulation in HFSS and measurements. Analyses of the results are showed here.

Chapter 4 draws the conclusion of this work.



## **CHAPTER 2 The Bandpass Filter Design**

### **Theory**

There are many traditional bandpass filter structures, such as the end-coupled microstrip bandpass filter, interdigital bandpass filter. Since the parallel coupled-line microstrip filter was proposed by Cohn in 1958 [23], it has been widely used in microwave applications. Due to its strong advantages such as planar structure, simple synthesis procedures and fabrication facility, it becomes an important component in bandpass filter design. However, as the development of the mobile communication, these conventional parallel coupled-line filters are too large to insert into the mobile systems. Many approaches had been developed for miniaturizing the coupled line. In this chapter, the basic theory of this thesis that based on capacitive loading of diagonally short-ended coupled-line for miniaturizing will be introduced.

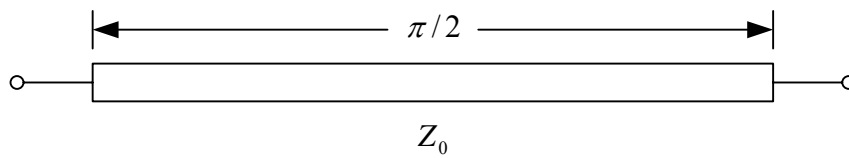
#### **2.1 Size reduction method**

As is well known, a quarter-wave transmission line can be miniaturized to a short line with electrical length of  $\theta$ , using combinations of shortened transmission line and shunt lumped capacitors proposed by Hirota [24] as shown in Fig. 2.1. The related equations are as follows,

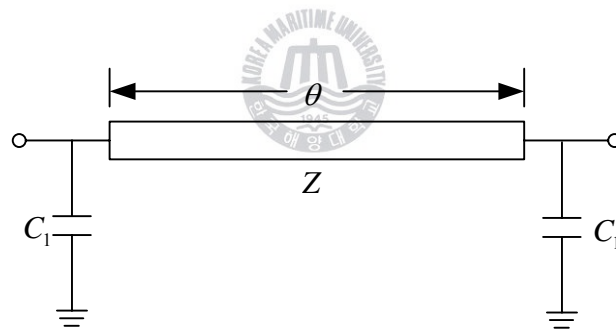
$$Z = Z_0 / \sin \theta \quad (2.1)$$

$$\omega C_1 = (1/Z_0) \cos \theta \quad (2.2)$$

where  $Z$ ,  $Z_0$ ,  $\theta$  and  $\omega$  are the characteristic impedance of the shortened transmission line, the characteristic impedance of the quarter-wavelength line, the electrical length of the shortened line.



(a)

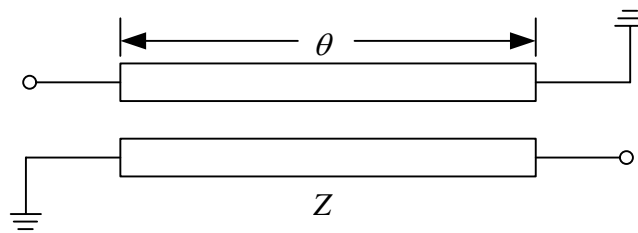


(b)

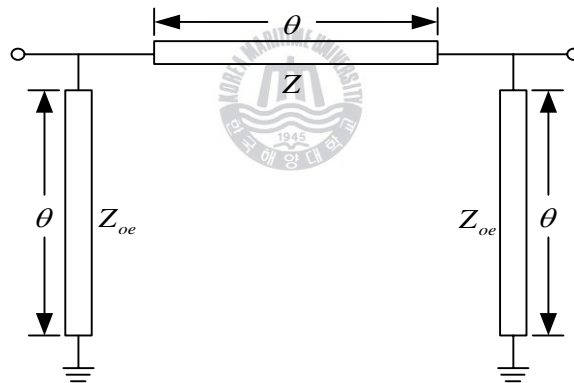
Fig. 2.1 Quarter-wave transmission line (a) and the shortened transmission line with lump capacitors(b).

From (2.1), it is clear that the characteristic impedance of the

shortened transmission line  $Z$  goes higher as the electrical length  $\theta$  goes smaller. When it is highly miniaturized, the impedance  $Z$  will too high to obtain. In order to reach very small electrical length up to several degrees, the coupled line component was adopted. Since it is easy to get a highly impedance through choosing the even-mode impedance approximate to the odd- mode impedance. A diagonally shorted coupled lines and its equivalent circuit [25] are shown in Fig. 2.2.



(a)



(b)

Fig. 2.2 Diagonally shorted coupled lines (a) and the equivalent circuit of the coupled lines (b).



The characteristic impedance of the diagonally shorted coupled lines can be represented by the even-mode and odd-mode characteristic impedance and thus is given by:

$$Z = \frac{2Z_{oe}Z_{oo}}{Z_{oe} - Z_{oo}} \quad (2.3)$$

Fig. 2.3 shows a shortened transmission line using Hirota's method with artificial resonance circuits. At the resonance frequency, the capacitance  $C_0$  and the inductance  $L_0$  cancel each other. So the equivalent circuit is the shortened quarter-wave transmission line using the Hirota's method as mentioned foregoing. At the resonance frequency, the following equation is satisfied:

$$\omega L_0 = \frac{1}{\omega C_0} \quad (2.4)$$

Compare the dotted box part in Fig. 2.3 and the equivalent circuit of the coupled lines in Fig. 2.2 (b). If the following equation is satisfied the dotted box part in Fig. 2.3 can be substituted by the equivalent circuit of the coupled lines. Then we get the substituted equivalent circuit as shown in Fig. 2.4.

$$\omega L_0 = Z_{oe} \tan \theta \quad (2.5)$$

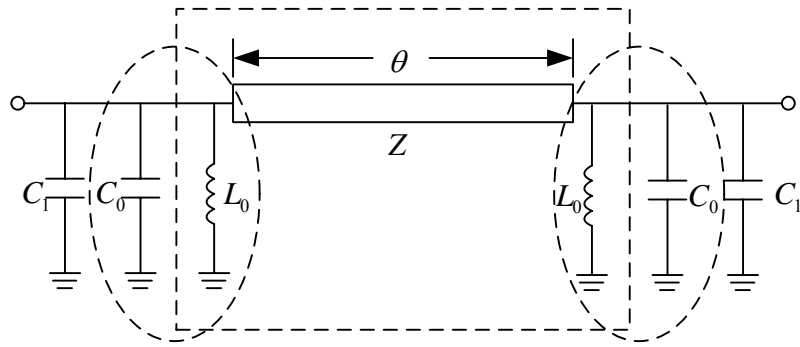


Fig. 2.3 A shortened transmission line with artificial resonance circuits.

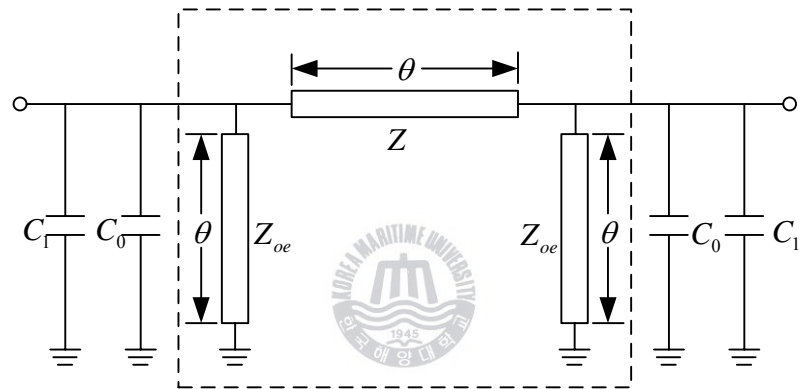


Fig. 2.4 The equivalent circuit substituted by the coupled lines' equivalent.

Finally, the two capacitors in each side of the Fig. 2.4 can combine mathematically, and the part in the dotted box is a diagonally shorted coupled line of Fig. 2.2 (a). The basic component of the filter can easily get. The structure of the diagonally miniaturized coupled lines with lumped capacitors appears as shown in Fig 2.5. And the relative equations

are as follows:

$$C = C_0 + C_1 \quad (2.6)$$

$$C_1 = \frac{\cos\theta}{\omega_0 Z_0} \quad (2.7)$$

$$C_0 = \frac{1}{\omega_0^2 L_0} = \frac{1}{\omega Z_{oe} \tan\theta} \quad (2.8)$$

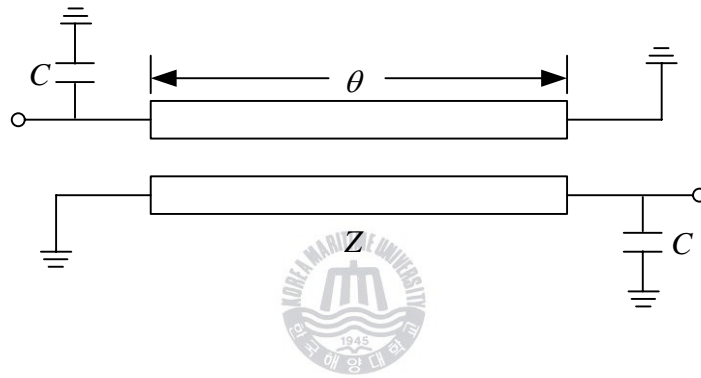


Fig. 2.5 The final equivalent circuit of the miniaturized quarter-wave transmission line.

This is the basic component of the proposed bandpass filter in this paper.

## 2.2 The two-stage filter

As we know, two-stage filter has many advantages compared to one

stage filter such as the improved flatness in the passband which increases the immunity against the perturbation of center frequency because of fabrication. In addition, two stage filters are always matched in the input and output port regardless of any fabrication error if two filters have same characteristic. Fig. 2.6 shows the two-stage filter. The process is as follows:

$$Z_{in1} = (Z_0')^2 / Z_0 \quad (2.9)$$

$$Z_{in} = \frac{(Z_0')^2}{(Z_0')^2 / Z_0} = Z_0 \quad (2.10)$$

Equation (2.9) shows the input impedance  $Z_{in1}$  at terminal of the second filter.  $Z_0'$  is the impedance of the transmission line,  $Z_0$  is the characteristic impedance.

As shown in equation (2.10), the input impedance of the two stage filter  $Z_{in}$  is equal to  $Z_0$ , that is, the two stage filter is matched automatically.

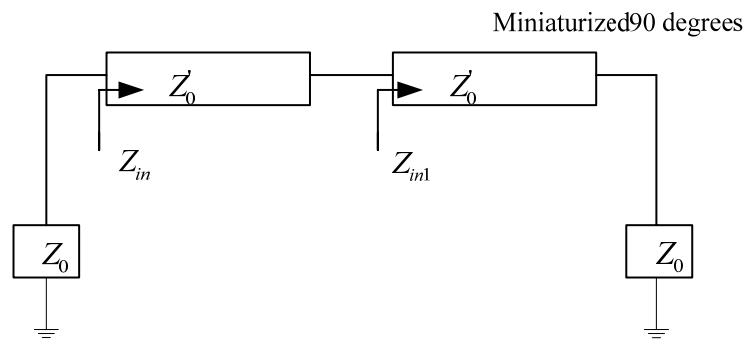


Fig. 2.6 The two-stage bandpass filter

### 2.3 The inter-stage signal line enhancement method

The inter-stage signal line between two filters is very important because there is some coupling between two resonators. However, in the CMOS process the coupling is even more severe. An extra ground plane is inserted into below the signal line to enhance the performance of the filters. In the next chapter, both the simulated and measured results will be plotted to show the different performances between the filters with extra ground plane and the ones without.

## **CHAPTER 3 The Simulation , fabrication and results analysis**

In this chapter, the enhancement method of the inter-stage line of the two-stage bandpass filter will be described based on theoretical circuit analysis. The performance of the innovative filters will be compared to the original ones. And the center frequency shifts will be theoretically proven to be caused by transmission losses and quality factors in the lossy distributed inductor of the shunt resonator.

### **3.1 The inter-stage signal line improvement**

For the actual circuits, an inter-stage part is very important because there is some coupling between two resonators. Fig. 3.1 shows an extremely miniaturized two-stage bandpass filter with a small transmission line in the middle which connects two resonators. It has been proved by [26] that the inter-stage transmission line is indispensable and the filtering characteristics get better as the line length is longer. However we pursue a compact size, so we have to make a tradeoff between the size and good performance.

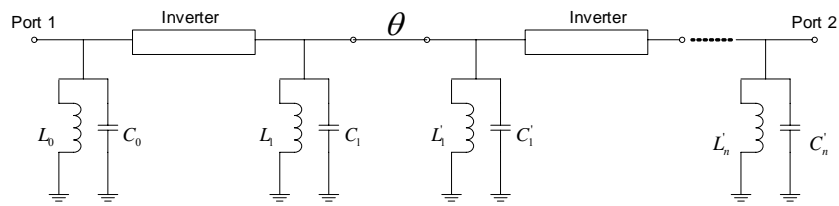


Fig. 3.1 An extremely miniaturized two-stage bandpass filter..

The structure of the BPF using the CMOS process is shown in Fig. 3.2. The Si substrate is used as the substrate to implement the RF CMOS process. A multi-layered circuit is constructed on the substrate with ground pillars arranged at both sides of a coupled line to avoid the coupling to other components. The oxide is used as the insulator inserted into the structure to prevent a current from flowing down.

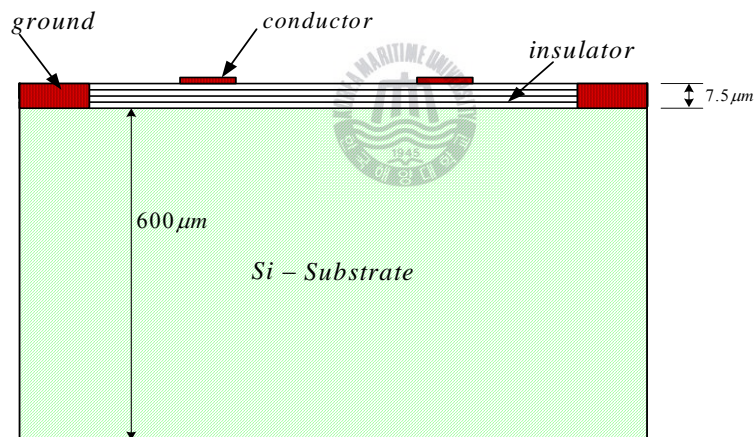
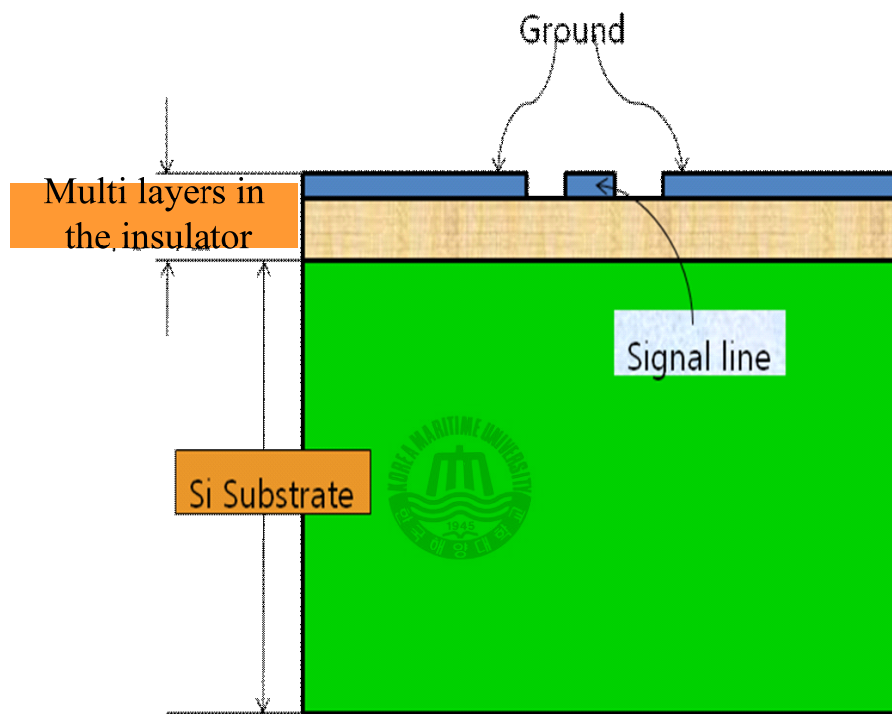


Fig. 3.2 The series resistance is substituted by the shunt conductance.

Fig. 3.3 (a) shows cross-sectional views illustrating the connection part of the original BPFs. The ground pillars arranged at both sides of the connecting line, so that the coupling can be effectively avoided. However, interference between two filters in the two-stage filter is very critical. If an extra ground plane is inserted under the line, the coupling will decrease further, and accordingly the performance of the filter should be better theoretically. The improvement is shown in Fig. 3.4 (b).



(a)



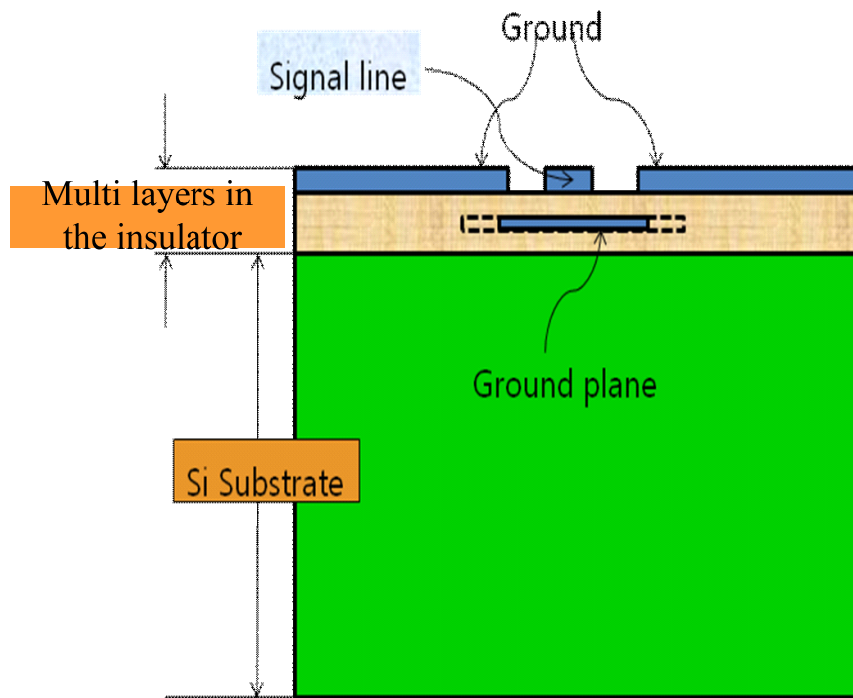


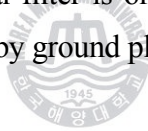
Fig. 3.3 The inter-stage signal line of the 2-stage bandpass filter (a) without ground plane (b) with ground plane.

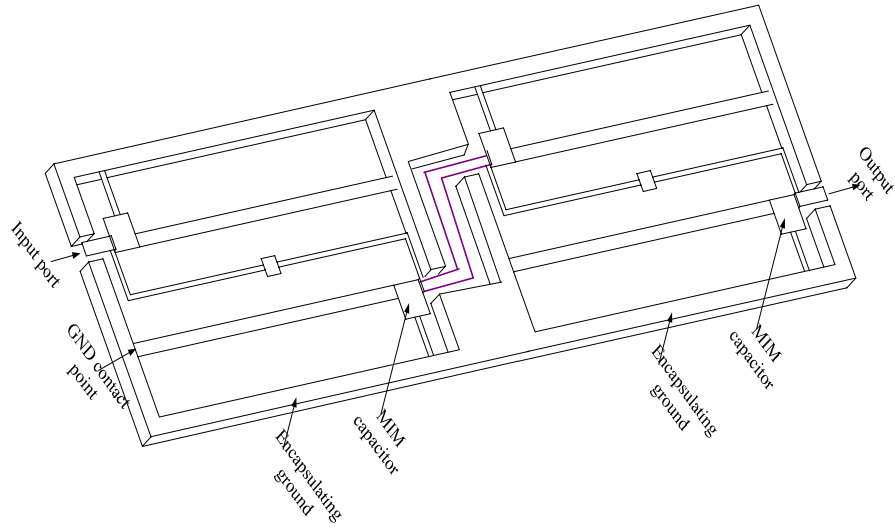
### 3.2 Simulation and fabrication

To verify the approaches both the original and the improved cascade miniaturized coupled line BPFs were considered with 1 and 6 layers, respectively. The structures of the filter with only inter-stage line and with

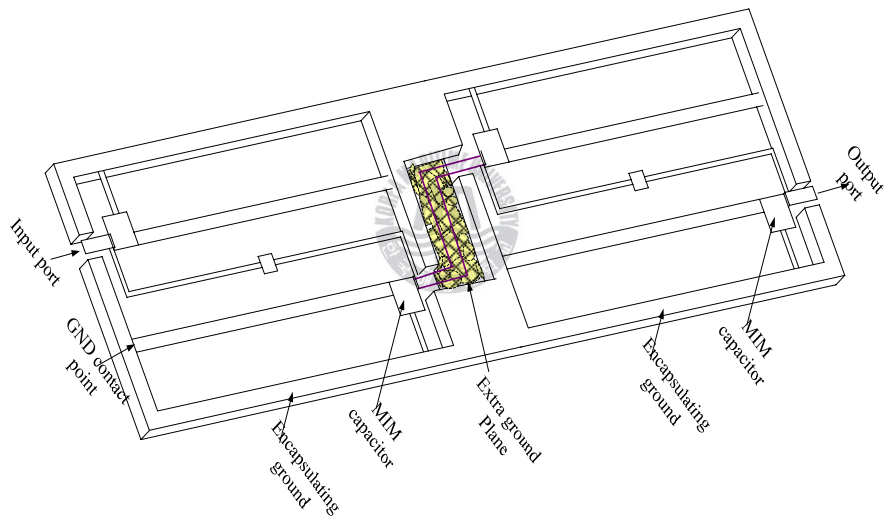
extra ground below the signal line are shown in Fig. 3.4. Firstly, a one stage bandpass filter is designed at 5.5 GHz. For the BPF with one layer, a coupled line of  $7^\circ$  electrical length is used. The coupled line width is 20  $\mu\text{m}$ , the transmission line length is 570  $\mu\text{m}$  and the separation between the two coupled lines of 140  $\mu\text{m}$  is used to provide input/output impedance matching to the system impedance  $Z_0 = 50 \Omega$ . The six layers filter also has a 20  $\mu\text{m}$  line width, 570  $\mu\text{m}$  line length, and 140  $\mu\text{m}$  coupled line separation. Then, two same one stage filters with 1 and 6 layers are cascaded, respectively. This technology is well explained by [27]. The thickness of the signal line is 2.34 $\mu\text{m}$ , and the thickness of the extra ground plane inserted into below the signal line is 1.91 $\mu\text{m}$ .

These filters have been fabricated on a 10  $\Omega\text{cm}$  bulk silicon substrate with aluminum metal layers. The total die area, including the ground plane surrounding the integrated BPF, is 1440  $\mu\text{m} \times 410 \mu\text{m}$ . Photograph of the BPFs with 6 layers are shown in Fig. 3.5. In Fig. 3.5 (a) the connection part of the original filter is only the transmission line and in Fig.3.5 (b) the line is covered by ground plane



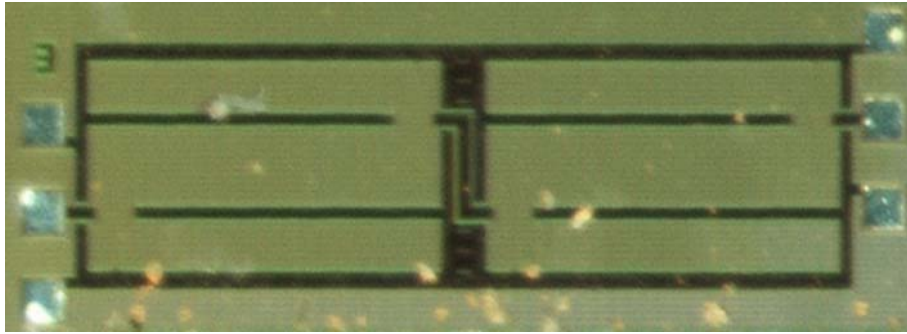


(a)

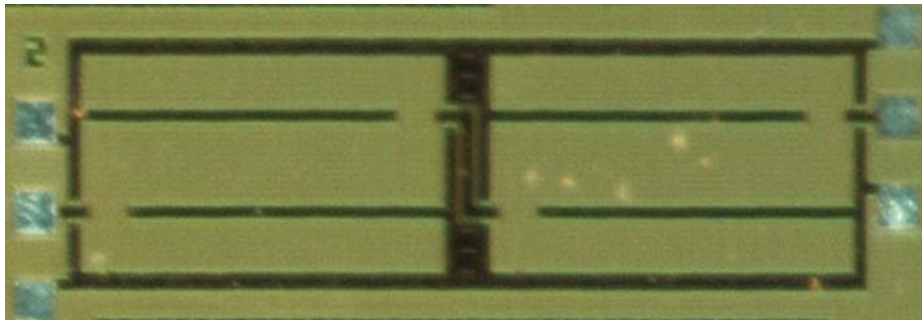


(b)

Fig. 3.4 Structure of the two-stage bandpass filters (a) the original filter without ground plane (b) the improved with ground plane.



(a)



(b)

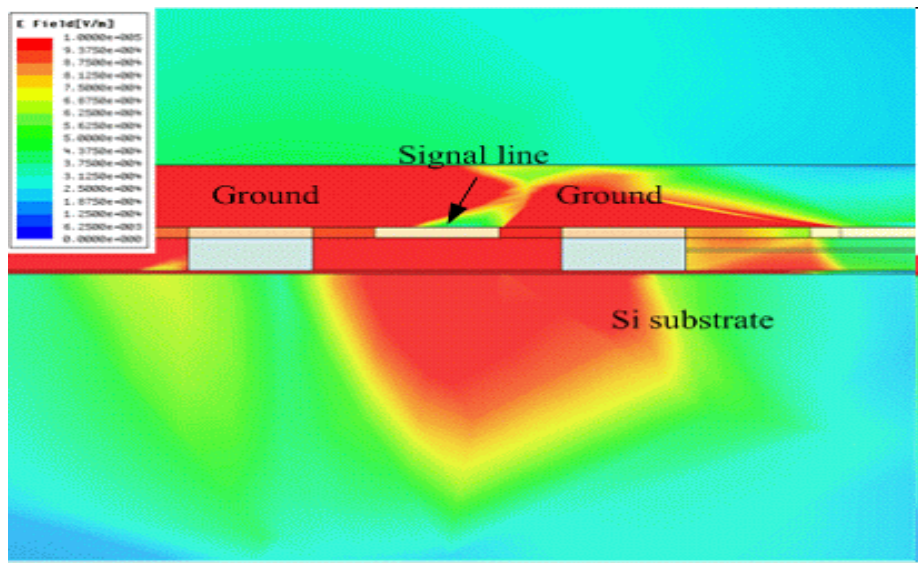
Fig. 3.5 Photograph of the fabricated six-layer bandpass filters with 6 layers (a) the original filter without ground plane (b) the improved with ground plane.

The connection part of the bandpass filter is based on coplanar waveguide (CPW) structure. Before describing the result of the filters we compare the two connection structures to gain some insight into the new design. Fig. 3.6 shows the electrical (E) distributions for the original structure and the improved with extra ground plane. Fig. 3.7 is the two connection parts with vector electrical distributions. The waveguides become lossy due to the parasitic coupling between the signal line and the substrate. As shown in Fig. 3.6(a), the electric field lines clearly penetrate

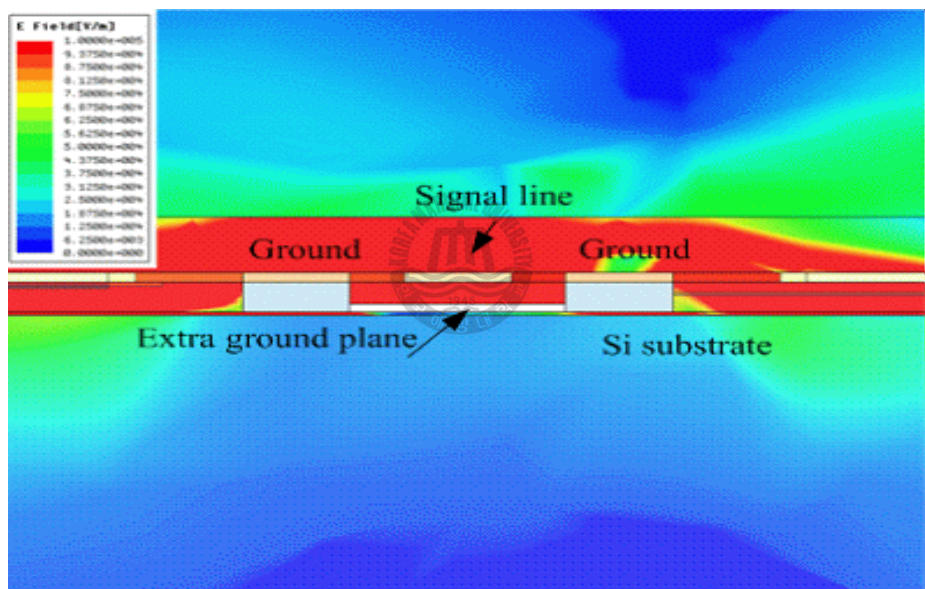
through the substrate and distributed in a nonuniform area. This will affect the performance of the filter. After inserting an extra ground plane shielding the signal line, the electric field penetration through the substrate is completely eliminated as shown in Fig. 3.6 (b). The electric field distributed in uniformly under the signal line. Fig. 3.7 shows the same distribution. Simulation and measured results will be plotted to verify it.

The simulated results of the circuit with one-layer and six-layer coupled lines are plotted in two figures, respectively. As shown in Fig. 3.8 (a), with 1 layer, the result of the original circuit without extra ground plane is distorted at 4.3 GHz because of the severe coupling while the improved one with extra ground plane has a normal bandpass filter shape. The insertion loss of the innovative filter is -4.13dB at its resonant frequency. This is an improvement of 1.79dB compared with the original one, which has an insertion loss of -5.92 at resonance. In Fig. 3.8 (b), the result of the original circuit without extra ground plane is distorted at 4.2 GHz while the improved one with extra ground plane has a normal bandpass filter shape. The insertion loss of the innovative filter with 6 layers is -2.3dB at its resonant frequency while the original one has an insertion loss of -5.67 at resonance. This is an improvement of 3.37dB.

Fig. 3.9 plotted the measured result of the 6-layer circuit. The circuit without extra ground plane was distorted at 4.7GHz because of the severe coupling while the approved one with extra ground plane had a normal bandpass filter shape. Apparently, the improved BPF with extra ground plane under the connecting line has advantage over the typical one both with 1 layer and 6 layers.

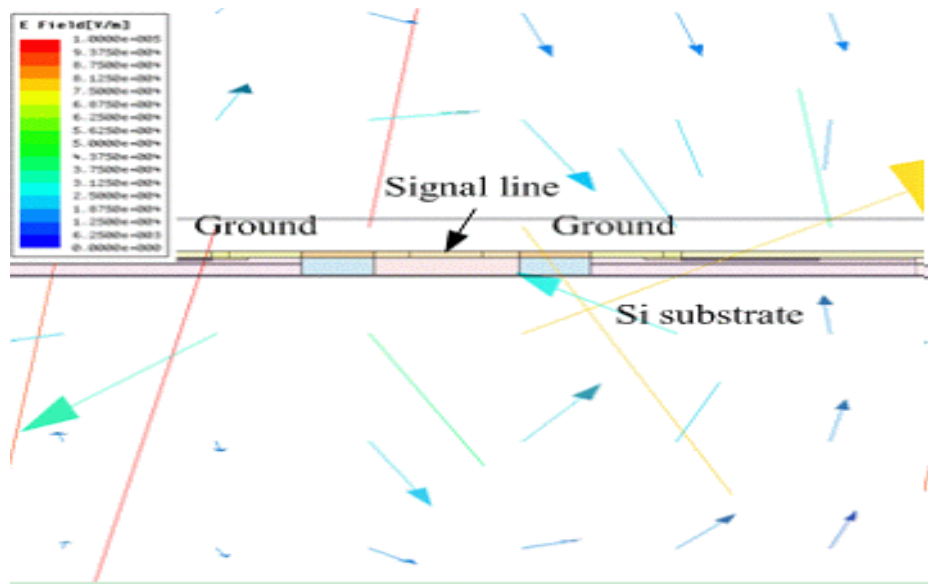


(a)



(b)

Fig. 3.6 Electric field distributions for original connection part (a) and improved connection part (b).



(a)

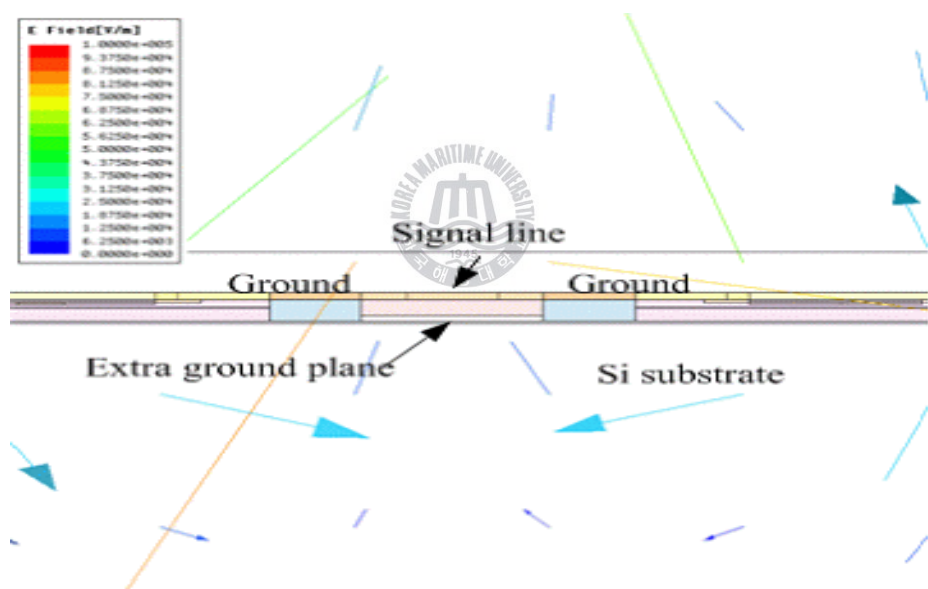
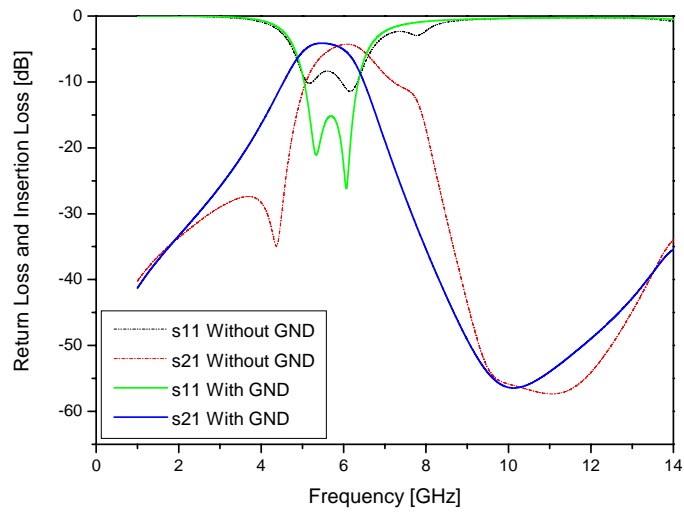
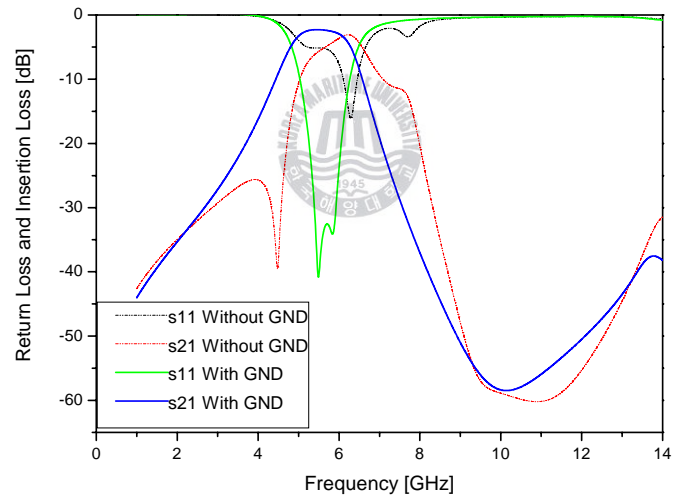


Fig. 3.7 Vector electric field distributions for original connection part (a) and improved connection part (b).



(a)



(b)

Fig. 3.8 The simulated results of the circuits with (a) 1 layer and (b) 6 layers.



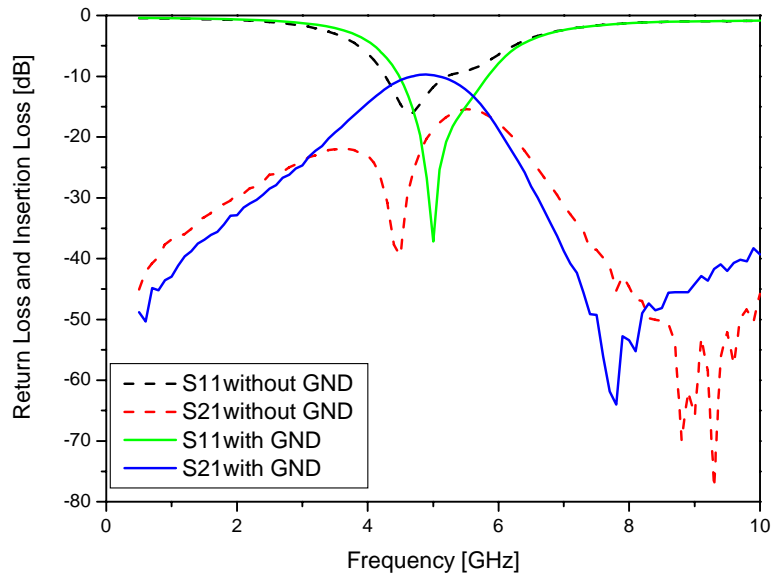


Fig. 3.9 The measured results of the circuits with 6 layers.



### 3.3 The quality factor effect on the resonance frequency shift

The BPF using a shunt resonator and a section of high-impedance transmission line is shown in Fig. 2.3. For the ideal BPF, we can set the conductivity of the substrate to zero and transmission line to lossless.

The resonator in Fig. 2.3 has a resonance frequency as follows:

$$\omega_r = \sqrt{\frac{1}{L_0 C_0}} = \omega_0 \quad (3.1)$$

where  $\omega_0$  is the center frequency.

Equation (3.1) shows that the resonance frequency  $\omega_r$  is equal to the center frequency  $\omega_0$  as expected, and the corresponding Q factor is infinity.

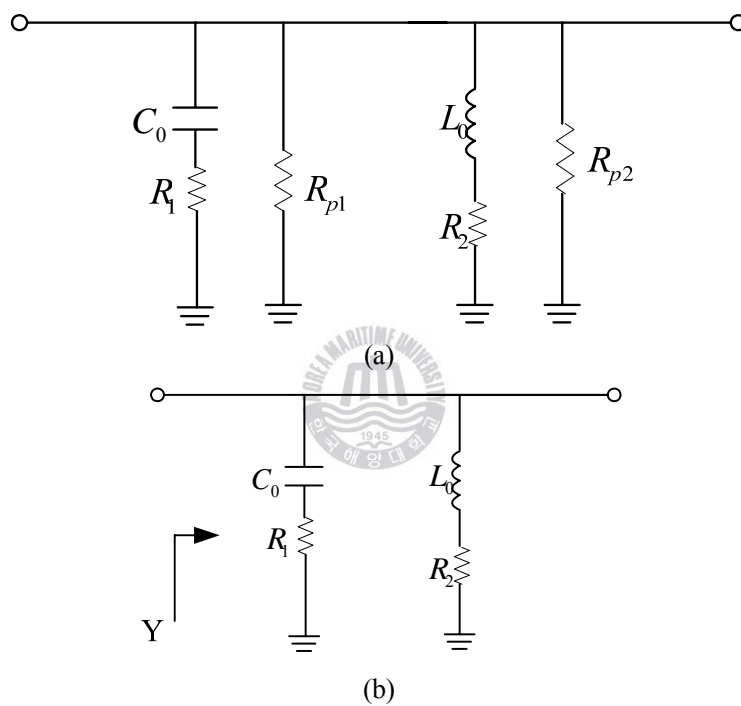


Fig. 3.10 The Equivalent circuit of the resonator

However, the substrate's loss effect is actually too severe to be ignored as the silicon substrate is inherently lossy and the electrical field

tends to leak into it. Although the exact equivalent circuit of the distributed inductor is complicated, we assume that the inductor loss is mainly due to the series resistance  $R_2$ , as shown in Fig. 3.10 (a), the equivalent circuit of the resonator, because the resistance  $R_{p1}$ ,  $R_{p2}$  of the parallel part does not change the resonant frequency of shunt resonance. Fig. 3.10 (b) is the simplified circuit of Fig. 3.10 (a) for modeling the resonance frequency deviation. For the MIM capacitor, an equivalent series resistance  $R_1$  exists in the MIM circuit model and a maximum Q of about 80 was reported [28].

The resonator in Fig. 3.10 (b) has the following Y admittance:

$$\begin{aligned}
 Y &= \frac{1}{R_2 + j\omega L_0} + \frac{1}{\frac{1}{j\omega C_0} + R_1} \\
 &= \frac{R_2 - j\omega L_0}{R_2^2 + (\omega L_0)^2} + \frac{j\omega C_0 (1 - j\omega R_1 C_0)}{1 + (\omega R_1 C_0)^2}
 \end{aligned} \tag{3.2}$$

The imaginary part of equation (3.2) equals to zero for resonance,

$$\frac{-j\omega L_0}{R_2^2 + (\omega L_0)^2} + \frac{j\omega C_0}{1 + (\omega R_1 C_0)^2} = 0 \tag{3.3}$$

The resonance frequency is derived from equation (3.3)

$$\omega_r = \frac{\sqrt{1 - \frac{C_0}{L_0} R_2^2}}{\sqrt{L_0 C_0 - (R_1 C_0)^2}} \tag{3.4}$$

From equation (3.4), the resonance frequency of the circuit in Fig. 3.10 (b) using the quality factors is expressed as follows:

$$w_r = w_0 \frac{\sqrt{1 - \frac{1}{Q_L^2}}}{\sqrt{1 - \frac{1}{Q_C^2}}} \quad (3.5)$$

where  $Q_L$  is the quality factor of the distributed inductor ,

$$Q_L = \frac{w_0 L_0}{R_2} \quad (3.6)$$

$Q_C$  is the quality factor of the MIM capacitor ,

$$Q_C = \frac{1}{w_0 R_1 C_0} \quad (3.7)$$

The corresponding operating resonance frequency  $w_r$  in equation (3.5) will be smaller than the center frequency  $w_0$  of the lossless circuit. In Fig. 3.11, the logarithm of  $\frac{\Delta w}{w_0}$  versus  $Q_L$  factor is plotted. Three kinds of curves are showed at  $Q_C = 40, 60, \text{ and } 80$ , respectively. As  $Q_C$  increases as shown in Fig 3.11,  $\log \frac{\Delta w}{w_0}$  increases. This trend is to be notable as not to be expected. When  $Q_C$  is equal to  $Q_L$  in Fig. 3.11,  $w_r$  becomes  $w_0$  and  $\frac{\Delta w}{w_0}$  is zero.

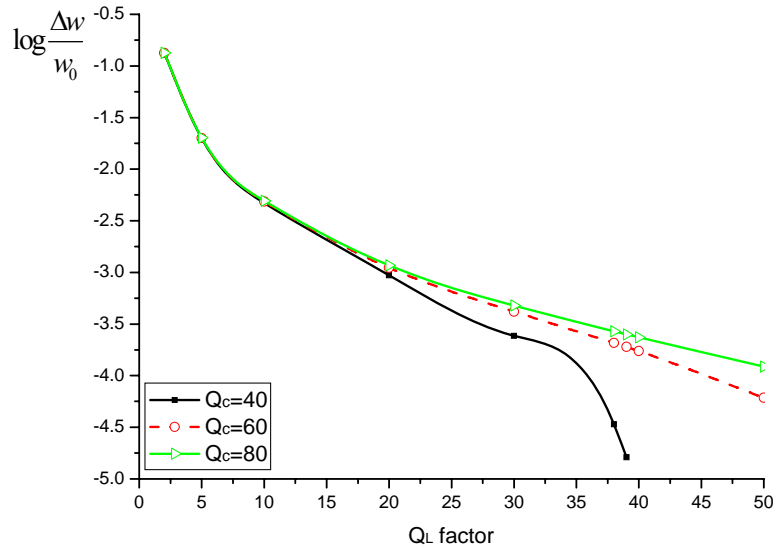
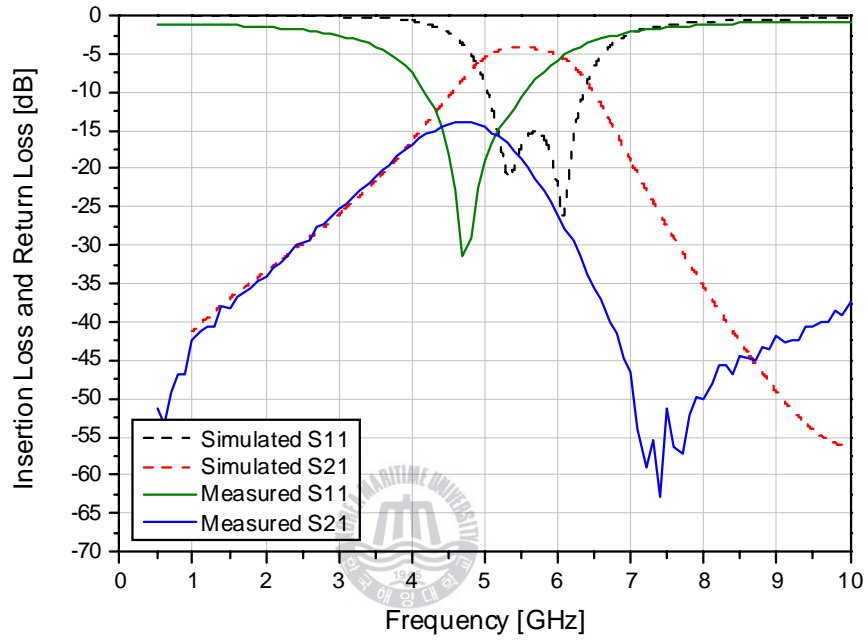


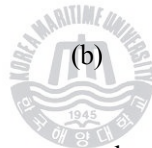
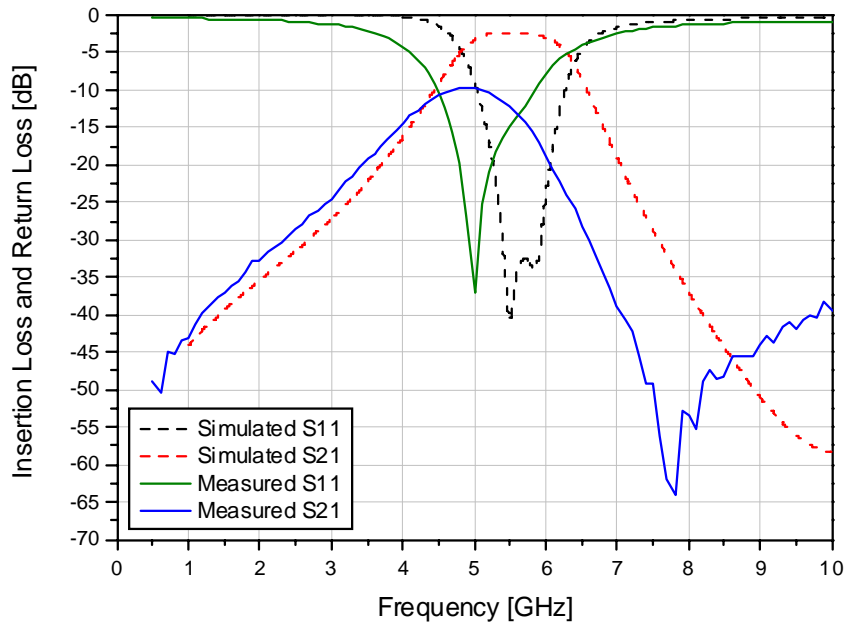
Fig. 3.11 The logarithm of  $\frac{\Delta w}{w_0}$  versus the  $Q_L$  factor

In Fig. 3.12, the simulated and measured results of the improved filter with one-layer and six-layer coupled lines are plotted. The  $Q_L$  factors of the BPF were found to be 4.9 and 14.8 for the one-layer and six-layer filters, respectively. The  $Q_L$  factor of the six-layer BPF circuit was better than that of the one-layer circuit. The simulated and the measured results are shown in Fig. 3.12. The dotted line was electromagnetically simulated by HFSS (Ansoft). The measured center frequency of the one-layer coupled lines BPF moved from 5.5 GHz to 4.7 GHz with 0.8 GHz shift as shown in Fig. 3.12 (a), whereas in Fig. 3.12 (b), the measured center frequency of the six-layer circuit moved from 5.5 GHz to 5 GHz with 0.5 GHz shift. Both of them have the center frequency shifting to the lower frequency after fabrication. According to

the simulation and measured results, the higher the  $Q_L$  factor, the less the center frequency shifts.



(a)



(b)  
 Fig. 3.12 The simulated and the measured results of the improved circuit with one-layer coupled lines (a) and six-layer coupled lines (b)

## CHAPTER 4 Conclusion

A novel two-stage coupled lines bandpass filter are proposed in this paper. The proposed filter is based on the structure of capacitive loading of the parallel short-ended coupled-line, which is a relatively simple mean of reducing the coupled-line electrical length that usually plays a decisive role to the filter size. The proposed filter with an extra ground plane inserted into below the signal line between two filters in the multilyers has an improved performance, since the ground plane can prevent the unwanted coupling between two filters from operating each other. In addition, the greater difference between the simulation and measurement of the bandpass filters in CMOS fabrication has been analyzed. The filters have suffered from inherent losses with silicon substrate and conductor losses. These losses are inclined to cause the center frequency to shift to the lower frequency. It is theoretically proven that the center frequency shifts is caused by transmission losses and quality factors in the lossy distributed inductor of shunt resonator of the coupled lines BPF.

The filters based on the MagnaChip CMOS procedures were fabricated. Both single layer coupled line filter and 6 layers coupled lines filter are included. It is proved that the improved filter with ground plane below the signal has better performance than the one with only signal line. With 1 layer, the insertion loss of the innovative BPF at its resonant frequency is -4.13 dB. This is an improvement of 1.79dB compared with the original BPF, which has an insertion loss of -5.92dB at resonance. The



insertion loss of the innovative filter with 6 layers is -2.3dB at its resonant frequency while the original one has an insertion loss of -5.67 at resonance. This is an improvement of 3.37dB. The approach is very novel and verified effective. Following the trend this approach to on-chip BPF implementation is likely to become even more attractive and competitive in the future.



## References

- [1] S. J. Fiedziuszko, "Dual-mode dielectric resonator loaded cavity filters," *IEEE Trans., Microw. Theory Tech.*, vol. 82, no. 9, pp. 1311–1316, Sep. 1982.
- [2] J. A. Curits and S. J. Fiedziuszko, "Miniature dual mode microstrip filters," *IEEE Trans., Microw. Theory Tech., Digest*, vol.2, pp. 443–446, Jul. 1991.
- [3] C. Wang, K. A. Zaki, and A. E. Atia, "Dual-mode conductor-loaded cavity filters," *IEEE Trans., Microw. Theory Tech.*, vol. 45, no. 8, pp. 1240–1246, Aug. 1997.
- [4] J. S. Hong and M. J. Lancaster, "Theory and experiment of novel microstrip slow-wave open-loop resonator filters," *IEEE Trans. Microw. Theory Tech.*, vol. 45, no. 12, pp. 2358–2365, Dec. 1997.
- [5] J. S. Hong and M. J. Lancaster, "End-coupled microstrip slow-wave resonator filter," *Electronics Letters*, vol. 32, no. 16, pp. 1494-1496, 1 Aug. 1996.
- [6] C. W. Tang, Y. C. Lin and C. Y. Chang, "Realization of transmission zeros in combline filters using an auxiliary inductively coupled ground plane," *IEEE Trans. Microwave Theory Tech.*, vol.51, no.10, pp.2112-2118, Oct., 2003.
- [7] A. Kundu and N. Mellen, "Miniaturized Multilayer Bandpass Filter with multiple Transmission Line Zeros", *IEEE MTT-S Int. Microwave Symp. Dig.*, pp. 760-763, June 2006.
- [8] J. S. Hong and M. J. Lancaster, "Cross-coupled microstrip hairpin resonator filters," *IEEE Trans. Microw. Theory Tech.*, vol. 46, no. 1, pp. 118-122, Jan. 1998.

- [9] J. T. Kuo and C. Y. Tsai, "Periodic stepped-impedance ring resonator (PSIRR) bandpass filter with a miniaturized area and desirable upper stopband characteristics" *IEEE Trans. Microw. Theory Tech.*, vol. 54, no. 3, pp. 1107-1112, Mar. 2006.
- [10] J. T. Kuo and E. Shih, "Microstrip stepped impedance resonator bandpass filter with an extended optimal rejection bandwidth," *IEEE Trans. Microw. Theory Tech.*, vol. 51, no. 5, pp. 1554-1559, May. 2003.
- [11] M. Makimoto and S. Yamashita, "Bandpass filters using parallel coupled strip-line stepped impedance resonators," *IEEE Trans. Microw. Theory Tech.*, vol. 28, no. 12, pp. 1413-1417, Dec. 1980.
- [12] B. Dehlink, M. Engl, K. Aufinger, H. Knapp, "Integrated Bandpass Filter at 77GHz in SiGe Technology", *IEEE Microwave and Wireless Components Letters*, vol.17, pp346-348, May 2007.
- [13] Y. Cao, R. A. Groves, X. Huang, N. D. Zamdmer, J. O. Plouchart, R. A. Wachnik, T. J. King, and C. Hu, "Frequency independent equivalent-circuit model for on-chip spiral inductors," *IEEE J. Solid-State Circuits*, vol. 38, no.3, pp. 419-426, Mar. 2003.
- [14] J. N. Burghartz et al., "RF circuit design aspects of spiral inductors on silicon," *IEEE J. Solid-State Circuits*, vol. 33, pp. 2028-2034, Dec. 1998.
- [15] C. P. Yue and S. S. Wong, "On-chip spiral inductors with patterned ground shields for Si-based RF ICs," *IEEE J. Solid-State Circuits*, vol. 33, No. 5, pp. 743-752, May 1998.
- [16] A. Niknejad and R. Meyer, "Analysis, design, and optimization of spiral inductors and transformers for Si RF ICs," *IEEE J. Solid-State Circuits*, vol. 33, pp. 1470-1481, Oct. 1998.
- [17] T. P. Wang and H. Wang, "High-Q Micromachined inductors for 10 to 30 GHz RFIC applications on low resistivity Si substrate", *Proc. of 36th European Microwave Conference*, pp. 56-59, 2006.
- [18] X. He and W. B Kuhn, "A 2.5GHz low power, high dynamic range self tuned Q enhanced LC filter in SOI", *IEEE J. Solid-State Circuits*, vol. 40, No. 8, pp. 579-586, August 2005.

- [19] X. He and W. Kuhn, "A 2.5GHz low-power, high dynamic range, self-tuned Q-enhanced LC filter in SOI," *IEEE Solid State Circuits*, vol. 40, no. 8, pp. 1618–1628, Aug 2005.
- [20] T. L. Brooks and P. M. VanPeteghem, "Simultaneous tuning and signal processing integrated continuous time filters: The correlated tuning loop," in *Proc. IEEE Int. Symp. Circuits and Systems*, 1989, pp. 651–654.
- [21] W. B. Kuhn, S. Elshabini-Riad, and F. W. Stephenson, "A new tuning technique for implementing very high Q continuous-time, bandpass filters in radio receiver applications," in *Proc. IEEE Int. Symp. Circuits and Systems*, 1994, pp. 5-257–5-260.
- [22] J. Brinkhoff and F. Lin, "Integrated filters for 60 GHz systems on CMOS," *IEEE Int. workshop on Radio Frequency Integration Technology*, Singapore, 2007, pp. 9–11.
- [23] S. B. Cohn, "Parallel-coupled transmission-line resonator filters," *IRE Trans.*, vol. MTT-6, no. 4, pp. 223-231, Apr. 1958.
- [24] T. Hirota, A. Minakawa and M. Muraguchi, "Reduced-size branch-line and rat-race Hybrids for uniplanar MMIC's," *IEEE Trans. Microwave Theory Tech.*, vol. 38, no. 3, pp. 270-275, 1990.
- [25] G. Matthaei, L. Young, E. M. T. Jones, *Microwave Filters, Impedance-Matching networks, and Coupling Structures*, Artech House, pp. 220.
- [26] I. H. Kang and H. Y. Xu, "An Extremely Miniaturized Microstrip Bandpass Filter", *Microwave Journal*, MAY, 2007.
- [27] I. Kang, S. Shan, X. Wang, Y. Yun, J. Kim, C. Park, "A miniaturized GaAs MMIC filter for the 5GHz band", *Microwave Journal*, vol. 50, pp. 88-94, Nov. 2007.
- [28] J. N. Burghartz, M. Soyuer, K. A. Jenkins, "Microwave inductors and capacitors in standard multilevel interconnect silicon technology", *IEEE Microwave Theory and Technologies*, vol. 44, No 1, pp. 100-104, Jan. 1996.

# Acknowledgement

I would like to acknowledge many people who have helped me in both my study and daily life during the past two years. It is impossible for me to finish this thesis without their supports and encouragements.

My greatest appreciation belongs to my advisor, Prof. In-Ho Kang. He is a creative and intelligent scholar. His strict research attitude and enthusiasm deeply impressed me. He taught me how to deal with problems, how to research new things. And I learned a lot from him in both science knowledge and working attitude which will influence my way to work and to study in the future. I feel very fortunate for his supervision and the words hardly express my gratitude to him. Without his help I couldn't complete my study in Korea.

I would also like to express my appreciation to the other professors of our department for their supports and guidance, who are Prof. Young Yun, Prof. Ki-Wan Kim. Thanks for the supports and guidance on my paper and their help during the two past years.

I also want to thank the members of the other lab of our department because of the help on my study life. Specially, the heartfelt thanks are due to the past member of the RF Circuit & System Lab, Mr. Hong-Chao Zhang, for lots of help and supports on the professional aspect. And Mr. Jun-Yong Park, who gives me a lot help in my Korea life. Additionally, I

want to thank all my friends in Korea Maritime University, for their unselfish help and emotional supports during the two years.

My special thanks belong to Prof. Ying-Ji Piao and Zheng-Li at Qingdao University of China. Without their recommendation, it is impossible for me to get the opportunity to study in Korea.

Finally, my thanks would go to my beloved family and my fiancée Yang-Yang for their continued love and strong supports throughout all these years. You are always the persons who believe in and encourage me in all my endeavors, which is a contributing factor to any success I may achieve. I feel great fortune to have you all accompany with me.

